BIOCHEMISTRY
including biophysical chemistry & molecular biology
Article

Biochemistry **2009,** *48,* 10405–10415 10405
DOI: 10.1021/bi900523q

Surface Plasmon Resonance Binding Kinetics of Alzheimer's Disease Amyloid β Peptide-Capturing and Plaque-Binding Monoclonal Antibodies[†]

Muthu Ramakrishnan,[‡] Karunya K. Kandimalla,[‡,§] Thomas M. Wengenack,[‡] Kyle G. Howell,[‡] and Joseph F. Poduslo*[,‡]

[‡]*Molecular Neurobiology Laboratory, Departments of Neurology, Neuroscience, and Biochemistry/Molecular Biology, Mayo Clinic College of Medicine, Rochester, Minnesota 55905, and* [§]*College of Pharmacy and Pharmaceutical Sciences, Florida A&M University, Tallahassee, Florida 32307*

Received March 26, 2009; Revised Manuscript Received September 22, 2009

ABSTRACT: Several different monoclonal antibodies (mAbs) have been actively developed in the field of Alzheimer's disease (AD) for basic science and clinical applications; however, the binding kinetics of many of the mAbs with the β-amyloid peptides (Aβ) are poorly understood. A panel of mAbs with different Aβ recognition sites, including our plaque-binding antibody (IgG4.1), a peptide-capturing antibody (11A50), and two classical mAbs (6E10 and 4G8) used for immunohistochemistry, were chosen for characterization of their kinetics of binding to monomeric and fibrillar forms of Aβ40 using surface plasmon resonance and their amyloid plaque binding ability in AD mouse brain sections using immunohistochemistry. The plaque-binding antibody (IgG4.1) with epitope specificity of Aβ(2−10) showed a weaker affinity (512 nM) for monomeric Aβ40 but a higher affinity (1.5 nM) for Aβ40 fibrils and labeled dense core plaques better than 6E10 as determined by immunohistochemistry. The peptide-capturing antibody (11A50) showed preferential affinity (32.5 nM) for monomeric Aβ40 but did not bind to Aβ40 fibrils, whereas antibodies 6E10 and 4G8 had moderate affinity for monomeric Aβ40 (22.3 and 30.1 nM, respectively). 4G8, which labels diffuse plaques better than 6E10, had a higher association rate constant than 6E10 but showed similar association and dissociation kinetics compared to those of 11A50. Enzymatic digestion of IgG4.1 to the $F(ab')_2$4.1 fragments or their polyamine-modified derivatives that enhance blood−brain barrier permeability did not affect the kinetic properties of the antigen binding site. These differences in kinetic binding to monomeric and fibrillar Aβ among various antibodies could be utilized to distinguish mAbs that might be useful for immunotherapy or amyloid plaque imaging versus those that could be utilized for bioanalytical techniques.

Alzheimer's disease (AD) is an incurable neurodegenerative disease that affects predominantly the aged population. While the disease pathology is not well understood, it is believed that the disease is associated with the accumulation of toxic amyloid peptides (Aβ) preferentially in the brain, which aggregate to form amyloid plaques and cerebrovascular deposits (*1*). In the monomeric form, Aβ peptide is randomly oriented without any ordered structure, but in the fibrillar form, it shows several different polymorphic structures (*2*−*4*). In the AD patient brain, these polymorphic Aβ fibrils are associated with dystrophic neurites, microglia, and astrocytes that are called neuritic amyloid plaques or with diffuse plaques that are the precursor forms of dense core plaques without dystrophic neurites. These diffuse plaques are found not only in AD patients but also in healthy aged humans free of any signs of dementia (*1*). While the mechanism of neuronal dysfunction is still not clear, it is widely believed that a particular form of amyloid protein assembly could impair memory in AD patients (*5*, *6*). Aβ peptide, therefore, is a primary diagnostic and therapeutic target for AD.

[†]Support was provided by Minnesota Partnership for Biotechnology and Medical Genomics and the Neuroscience Cores for MR Studies of the Brain from the National Institute of Neurological Disorders and Stroke (NS057091).

*To whom correspondence should be addressed: Departments of Neurology, Neuroscience, and Biochemistry/Molecular Biology, Mayo Clinic College of Medicine, 200 First St. SW, Rochester, MN 55905. Phone: (507) 284-1784. Fax: (507) 284-3383. E-mail: poduslo.joseph@mayo.edu.

It was reported previously that peripheral administration of mAbs in AD transgenic mice showed efficacy in reducing the size of the brain amyloid plaque burden (*7*). As a result, many different monoclonal antibodies have been developed for targeting Aβ peptides and are in different stages of clinical trials for immunotherapy in AD patients by major biopharmaceutical companies, with an emphasis on clearing the extracellular Aβ plaque deposits in AD patients and promoting behavioral improvements (*8*, *9*). However, fundamental differences have been observed with these mAbs, such as recognition of the Aβ antigen, affinity for Aβ, and the mechanism of action. Bard et al. (*7*) reported that an N-terminal antibody (3D6), which supposedly crosses the blood−brain barrier (BBB), clears parenchymal amyloid deposits presumably via microglial phagocytosis. DeMattos et al. (*10*) showed that a high-affinity Aβ peptide-capturing antibody (m266), which targets the central domain of Aβ but lacks binding to plaques, reduces the number of Aβ deposits from the brain by supposedly sequestering Aβ to the plasma and thereby altering the Aβ equilibrium between brain and circulating plasma. Recently, Seubert et al. (*11*) reported that this peptide-capturing antibody (m266) is not efficient in clearing plaques as it also increases the level of cerebrovascular amyloidosis, whereas a plaque-binding antibody, 3D6, is highly effective in reducing the plaque load present in the brain and cerebrovasculature.

Assessment of the therapeutic potential of anti-Aβ antibodies largely depends on expensive in vivo pharmacokinetic and

Published on Web 09/23/2009

pharmacodynamic experiments. Moreover, it is difficult to screen and define the required biochemical and biophysical properties of a potential antibody for immunotherapy through in vivo studies. In addition, most of these antibodies are not commercially available to researchers which would allow systematic studies to be conducted. Those antibodies that are commercially available for investigational purposes are also cost prohibitive for conducting immunotherapeutic preclinical trials. IgG4.1 is our own monoclonal antibody raised against fibrillar human Aβ42 peptide developed for therapeutic and diagnostic purposes for AD. Recently, we have demonstrated that the polyamine (p)-modified F(ab′)$_2$ fragment of IgG4.1 had increased BBB permeability of ~25- and ~50-fold compared to the native IgG4.1 or F(ab′)$_2$4.1 and successfully targeted amyloid plaques after intravenous administration (*12*, *13*). Obviously, increasing the delivery payload across the BBB even by a small fraction could have a great therapeutic impact, since only ~0.1−1% of therapeutic antibodies are present in CNS after the immunization. Compared to insulin, which undergoes receptor-mediated transcytosis, antibodies have a nearly 240-fold lower BBB permeability (*14*).

Apart from immunotherapy, monoclonal antibodies are also used extensively in basic science for bioanalytical purposes, such as an enzyme-linked immunosorbent assay (ELISA), to quantify Aβ peptides in tissues, plasma, and cerebrospinal fluid (*15*−*17*) and also to develop novel immune conjugates for diagnostic imaging (*12*, *18*). In this study, we have chosen a set of mAbs against Aβ peptides developed for Alzheimer's disease for different purposes: (1) a peptide-capturing antibody that captures soluble Aβ for bioanalytical techniques, (2) two mAbs for labeling diffuse and dense core amyloid plaques in tissue sections for immunohistochemistry techniques, and (3) a plaque binding antibody for diagnostic as well as therapeutic purposes. We characterized the binding of these mAbs to monomeric and fibrillar human Aβ40 using surface plasmon resonance (SPR) biosensor technology and their ability to bind diffuse and dense core plaques present in AD mouse brain sections using immunohistochemistry. We show that these mAbs have some fundamental differences in their biophysical interactions with different structures of monomeric and fibrillar Aβ40 and thus manifest different binding kinetics. The results are discussed in the context of choosing and developing these mAbs for specific needs for AD research. We have also studied the epitope mapping of IgG4.1 and demonstrated that the enzyme digestion of native IgG4.1 to F(ab′)$_2$4.1 preserved the antigen binding regions.

MATERIALS AND METHODS

Animals. Hemizygous transgenic mice (mouse strain C57B6/SJL, ID Tg2576) expressing mutant human amyloid precursor protein (APP695) (*19*) were bred in our mice colony at Mayo. These transgenic mice have been shown to exhibit parenchymal amyloid deposits by 12 months of age (*20*). The animals were housed in a virus-free, light- and temperature-controlled barrier environment. They were provided with free access to food and water. All procedures with animals were in strict accordance with National Institutes of Health Guide for the Care and Use of Laboratory animals and were approved by the Mayo Institutional Animal Care and Use Committee.

Preparation of Monomeric and Fibrillar Aβ40. Aβ40 peptide was obtained from Mayo Peptide Core Facility (Rochester, MN) in lyophilized form. The preparation of monomeric Aβ40 followed the procedures described by Bitan et al. (*21*) and Nichols et al. (*22*). The monomeric Aβ40 peptide was purified further using the method described by Nichols et al. (*22*). Briefly, monomeric Aβ40 was purified from lyophilized Aβ40 at a concentration of 4 μg/μL in HBS-EP buffer [0.01 M HEPES (pH 7.4), 0.15 M NaCl, 3 mM EDTA, and 0.005% P20] and bath sonicated for 40 s to obtain a clear solution. The sample was spun at 14000 rpm for 20 min and passed through a 0.2 μm filter to remove any large aggregates before injection of 200 μL of sample into the Superdex size exclusion column connected to an FPLC system. The concentration of purified monomeric Aβ40 was determined by measuring its absorbance at 280 nm and using the absorption coefficient of 1490. The Aβ40 concentration of 4 μg/μL was used for the consistent preparation of a monomeric Aβ40 solution from which various dilutions from 5 to 250 nM were made for SPR kinetic analysis. The size exclusion chromatogram of monomeric Aβ40 was reproducible and very similar to that reported previously (*21*, *22*). The purified monomer did not exhibit any fluorescence emission to thioflavin T (THT) excited at 450 nm which demonstrates the absence of β-sheet structures. In addition, we did not see any aggregation or fibrillar structure when the monomeric fraction was viewed under an electron microscope at high magnification (data not shown).

From monomeric Aβ40, the fibrils were grown using the following procedure. Approximately 1 mg of Aβ40 peptide was dissolved in 1 mL of PBS [10 mM phosphate buffer (pH 7.4)] and then bath sonicated for 40 s to obtain a clear solution. The sample was spun at 14000 rpm for 20 min and filtered through a 0.22 μm syringe. Then the sample was agitated at 250 rpm on an orbital shaker for 48 h at 37 °C to form Aβ40 fibrils. The fibrils grown under these condition show strong fluorescence emission to THT excited at 450 nm and exhibit mature fibrillar structure. The last two C-terminal residues of Aβ42 make the peptide more hydrophobic and less soluble than Aβ40. In addition, Aβ42 is known to forms fibrils rapidly compared to Aβ40, and hence, we restricted our studies only to Aβ40.

Instrumentation and Surface Preparation. SPR analyses were performed at 25 °C using Biacore 3000 optical biosensors with research grade CM5 chips (Biacore, Uppsala, Sweden). IgG4.1, raised against human fibrilar Aβ42, was obtained from Mayo Monoclonal Core Facility as described by Poduslo et al. (*13*). Other anti-amyloid antibodies, 4G8 (SIG-39220; Signet/Covance, Dedham, MA), 6E10 (SIG-39320; Signet/Covance), or a β-amyloid 1−40 antibody specific to the C-terminus (clone 11A50-B10; SIG-39140; Signet/Covance), were purchased from commercial vendors. Carboxymethylated CM5 chips were activated using 0.2 M *N*-ethyl-*N*′-(dimethylaminopropyl)carbodiimide (EDC) and 0.05 M *N*-hydroxysuccinimide (NHS). Pure monoclonal antibodies were immobilized at a density of ~2000 response units (RU) to study their binding kinetics with monomeric Aβ40. A nonspecific antibody (L227-IgG1κ antibody produced by mouse myeloma L227, catalog no. HB-96, ATCC, Manassas, VA) was immobilized at a similar density over the reference surface to control for nonspecific binding. A lower level of sonicated Aβ40 fibrils at a density of 9 or 60 Ru was immobilized to study the antibody binding kinetics with Aβ40 fibrils to minimize avidity effects. The residual activated carboxylic acid groups were quenched by blocking the surface with a 1 M ethanolamine hydrochloride solution. A plain CM5 surface (flow cell, Fc$_1$) which was activated and blocked by ethanolamine was used as a reference surface.

Kinetic Analysis of Aβ Monomers Binding to Immobilized Antibodies. Binding experiments were performed using

HBS-EP buffer [0.01 M HEPES (pH 7.4), 0.15 M NaCl, 3 mM EDTA, and 0.005% P20] as a running buffer. The binding sensorgrams were recorded by injecting different concentrations of freshly prepared Aβ40 monomers in HBS-EP buffer for 5 min at a flow rate of 30 μL/min over the immobilized antibody surface. The dissociation profile was monitored for 15 min, and then the surface was regenerated with 10 mM glycine HCl at pH 3.0. The activity of the immobilized antibody was not affected by the regeneration condition employed here, and the chips could be reused in further experiments. Before the kinetic experiments were performed, the surface antigen binding and regeneration conditions were optimized. To avoid any mass transfer effect, the experiments were performed at a high flow rate of 30 μL/min at 25 °C using freshly prepared Aβ40 monomers.

Kinetic Analysis of Antibodies Binding to Immobilized Sonicated Aβ40 Fibrils. Antibody kinetics with the Aβ fibrils may serve as a good in vitro model for studying the antibody interactions with amyloid plaques. However, the heterogeneous nature of fibrils limits this application in producing clean kinetic data. To minimize these complexities, the following procedure was employed: Aβ40 fibrils were grown as described above, and the long fibrils (86 μM) were sonicated in a glass tube using a bath sonicator for 2 min to break them into smaller fibrils. The sonicated fibrils were immobilized over the CM5 chip immediately after the sonication to avoid further aggregation of fibrils. To minimize the avidity effect, the sonicated fibrils were diluted in 10 mM sodium acetate at pH 4.0 and immobilized over the CM5 surface at very low density of 60 RU. This procedure allows the fibrils to spread easily and avoid crowded intermolecular interactions. A 10 μL aliquot of sonicated fibrils was mixed immediately with 200 μL of immobilization buffer (10 mM sodium acetate at pH 4.0), injected over the activated CM5 chip surface at a flow rate of 10 μL/min for 3 min, and then the unreacted carboxyl groups were blocked with ethanolamine. The binding sensorgrams were recorded by injecting antibody (33−200 nM) onto the immobilized Aβ40 fibril surface for 5 min at a flow rate of 30 μL/min using a reference surface (flow cell 1) which was activated and blocked with ethanolamine. The dissociation profile was monitored for ~15 min, and then the surface was regenerated with 10 mM glycine HCl buffer at pH 1.5.

Data Analysis. The kinetic constants of binding were obtained using a simple 1:1 Langmuir binding model shown below.

$$\text{analyte} + \text{ligand} \underset{K_d}{\overset{K_a}{\rightleftarrows}} \text{complex}$$

This model assumes the simplest situation of an interaction between analyte and immobilized ligand. The model is equal to the Langmuir adsorption isotherm developed by Irving Langmuir to describe the adsorption of molecules on a solid surface at a fixed temperature (*23*). The SPR raw data were analyzed using BIAevaluation (version 3.2) provided by Biacore Inc. (Uppsala, Sweden). After the background responses obtained from the control flow cells had been subtracted, the association and dissociation phases were fitted simultaneously using the global fit option, omitting any noisy data at the beginning and end of the analyte injection. In addition, the calculated affinity constant (K_D) obtained from the global fit was further validated by applying equilibrium steady state analysis. The K_D values calculated from both the methods matched closely. However, the global fit did not work well with the data obtained from immobilized Aβ40 fibrils. Hence, a local fit was employed at each concentration, and the average kinetic constants are reported in Table 1.

Labeling of Amyloid Plaques in APP Mouse and Human AD Brain Sections with IgG4.1, pIgG4.1, F(ab′)$_2$4.1, and pF(ab′)$_2$4.1. The polyamine (p) modification of IgG4.1 and F(ab′)$_2$4.1 was performed as described by Poduslo et al. (*13*). IgG4.1, pIgG4.1, F(ab′)$_2$4.1, or pF(ab′)$_2$4.1 was incubated in vitro with cryosections of brain from a 20-month-old APP transgenic mouse to test the ability of the antibodies to bind to amyloid plaques. The presence of the immunoglobulin or fragments was detected following the immunoperoxidase method developed to minimize nonspecific binding of mouse monoclonal antibodies in mouse tissue (MOM Peroxidase Kit, PK-2200, Vector Laboratories, Burlingame, CA). Briefly, 15 μm thick cryosections were lightly fixed with neutral-buffered 10% formalin for 5 min to prevent the tissue from disintegrating during the 2 day procedure. The sections were then washed with tap water three times for 5 min each and then twice with 0.3% Triton X-100 in PBS (PBST) for 5 min each. The endogenous peroxidase activity in the tissue was blocked by reaction with 0.3% H_2O_2 in PBST for 30 min. The sections were rinsed twice in PBST for 5 min each and then blocked for 60 min with MOM blocking solution in PBST according to the instructions. After being rinsed twice in PBST for 5 min each, the sections were equilibrated in MOM diluent (MOM Protein Concentrate in PBST) for 5 min and then incubated with 1.0 or 0.5 μg/mL immunoglobulin or fragment in MOM diluent overnight at 4 °C. For the sake of comparison, three standard anti-amyloid antibodies, 4G8 (SIG-39220; Signet/Covance), 6E10 (SIG-39320; Signet/Covance), or a β-amyloid 1−40 antibody specific to C-terminus (clone 11A50-B10, SIG-39140; Signet/Covance), were tested at the same dilutions. A control section was incubated in MOM diluent alone without the addition of an antibody. On the second day, sections were rinsed twice with PBST for 5 min each and then incubated with the biotinylated horse anti-mouse secondary antibody (MOM Peroxidase Kit) at a dilution of 1:250 for 45 min. After being rinsed twice in PBST for 5 min each, sections were incubated with ABC reagent (MOM Peroxidase Kit) for 45 min and then rinsed twice in PBS (without 0.3% Triton X-100) for 5 min each. Sections were reacted with Vector VIP peroxidase substrate (SK-4600, Vector Laboratories) for 1 min and then rinsed three times in tap water for 5 min each. Sections were rinsed three times in deionized water for 5 min each, dehydrated with successive changes of ethanol and xylene, and then placed on coverslips. As a control for the effects of polyamine modification on the binding of the antibodies and fragments to amyloid plaques and brain tissue, a nonspecific antibody (an anti-human Ia antigen IgG1κ antibody produced by mouse B lymphocyte hybridoma L227, catalog no. HB-96, ATCC), both native and polyamine-modified, was reacted with APP brain sections following the same immunohistochemical procedure described above.

Densitometry of IgG4.1, pIgG4.1, F(ab′)$_2$4.1, and pF(ab′)$_2$4.1 Labeling of Amyloid Plaques in APP Mouse Brain Sections. The intensity of the immunoreactivity of the anti-amyloid antibodies was quantitated on amyloid plaques as a measure of affinity. Grayscale images of APP mouse frontal cortex were taken in two hemispheres in two adjacent sections incubated with the anti-amyloid antibodies at two different concentrations. Using image analysis software (Axiovision, Carl Zeiss, Thornwood, NY), the intensity of each plaque was measured. The values were normalized against the background illumination intensity of an ROI measured on the empty slide immediately adjacent to the brain section, expressed as ratios of less than 1.0. Lower intensities and ratios represent darker levels

Table 1: Kinetic Constants of Various Antibodies and Fragments with Monomeric and Fibrillar Forms of Aβ40 Obtained via SPR

analyte[a] injected	ligand[b] immobilized	k_a ($\times 10^4$ M^{-1} s^{-1})	k_d (s^{-1})	K_D ($\times 10^{-9}$ M)	χ^2
Aβ40 monomer	6E10	3.8	8.48×10^{-4}	22.3	1.04
Aβ40 monomer	4G8	26.8	0.81×10^{-4}	30.1	0.81
Aβ40 monomer	11A50	24.7	0.80×10^{-4}	32.5	0.66
Aβ40 monomer	IgG4.1	7.2	0.037	512.0	0.35
Aβ40 monomer	F(ab′)$_2$4.1	3.7	0.018	491.0	2.48
6E10	Aβ40 fibril	20.8	2.91×10^{-4}	1.40	2.50
11A50	Aβ40 fibril	no interaction could be reliably measured			
IgG4.1	Aβ40 fibril	18.5	2.80×10^{-4}	1.50	6.61
F(ab′)$_2$4.1	Aβ40 fibril	22.4	5.34×10^{-4}	2.38	3.50
pIgG4.1	Aβ40 fibril	28.7	2.98×10^{-4}	1.04	15.40
pF(ab′)$_2$4.1	Aβ40 fibril	15.8	3.35×10^{-4}	2.12	4.49

[a]Analyte refers to the sample that was injected over the immobilized chip surface. [b]Ligand refers to the sample that is covalently linked to the sensor chip surface.

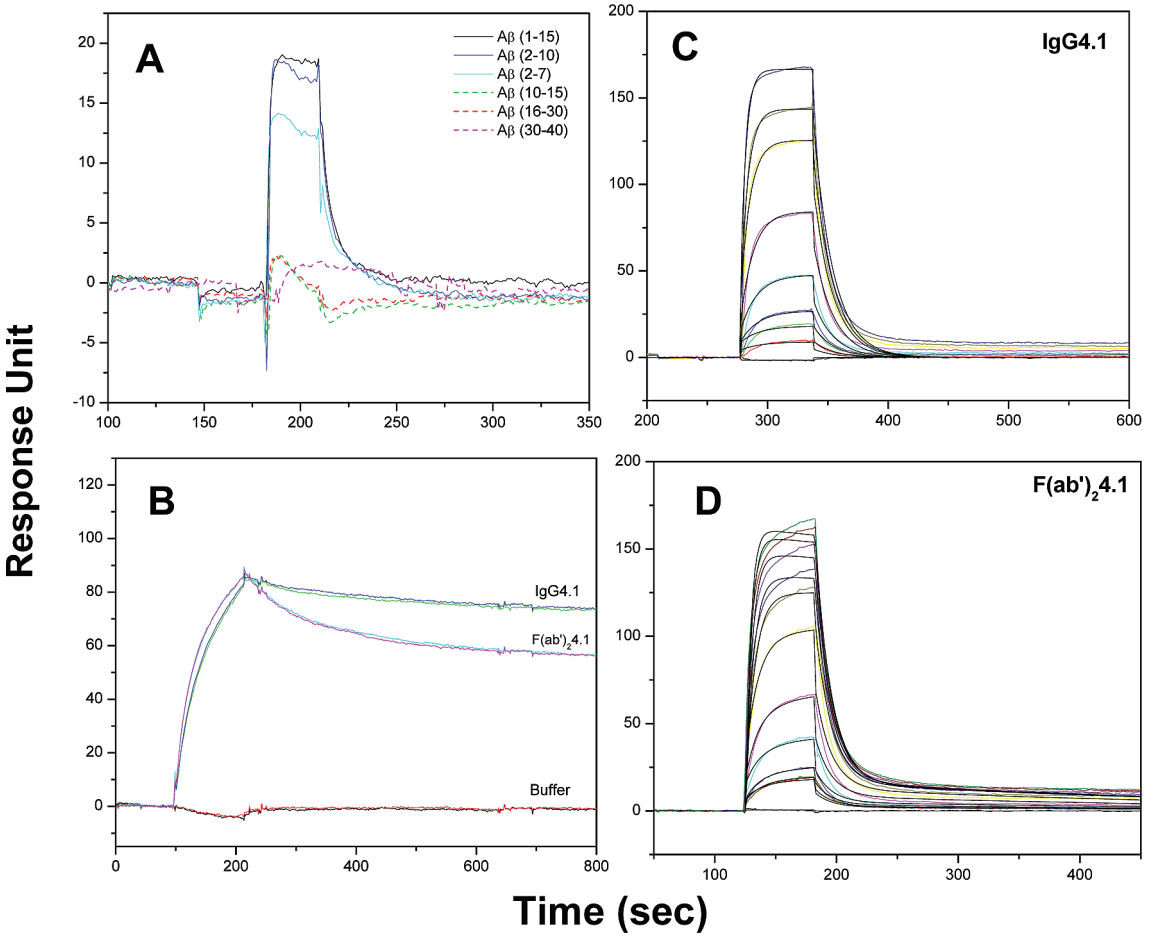

FIGURE 1: Epitope mapping of IgG4.1 and kinetics of ficin-digested antibody fragment. (A) SPR sensorgrams of IgG4.1 binding to different Aβ fragments demonstrating the epitope binding region of IgG4.1 as the N-terminal region of the Aβ peptide from 2 to 10. (B) Sensorgram of immobilized fibrillar Aβ40 binding to IgG4.1 and F(ab′)$_2$4.1 at 200 nM. (C and D) Sensorgrams of immobilized IgG4.1 (C) and immobilized F(ab′)$_2$4.1 (D) binding to monomeric Aβ40 at 30−3000 nM. The sensorgrams are shown as colored lines, and the fits are shown as black lines. This demonstrates that the enzyme digestion of the antibody to F(ab′)$_2$4.1 fragments does not alter the binding region.

of gray and black and hence higher levels of immunoreactivity and antibody binding.

RESULTS

Epitope Mapping of IgG4.1. Surface plasmon resonance was used to map the epitope binding region of IgG4.1. Different fragments of Aβ peptides were injected at a concentration of 100 nM for 60 s at a flow rate of 30 μL/min over the immobilized IgG4.1 surface. As shown in Figure 1A, IgG4.1 binds specifically to N-terminal Aβ peptides Aβ1−15, Aβ2−10, and Aβ2−7 but not to Aβ10−15, Aβ16−30, or Aβ30−40. The binding of Aβ1−15 is nearly identical to the binding of Aβ2−10, whereas Aβ2−7 shows a weakened binding response without altering the shape of the curve. The reduced level of binding may arise from the mass differences between the peptides. These data reveal that IgG4.1 has an epitope specificity for Aβ(2−10).

Kinetics of the Ficin-Digested Antibody Fragment. Ficin is an enzyme widely used to cleave antibodies near the hinge

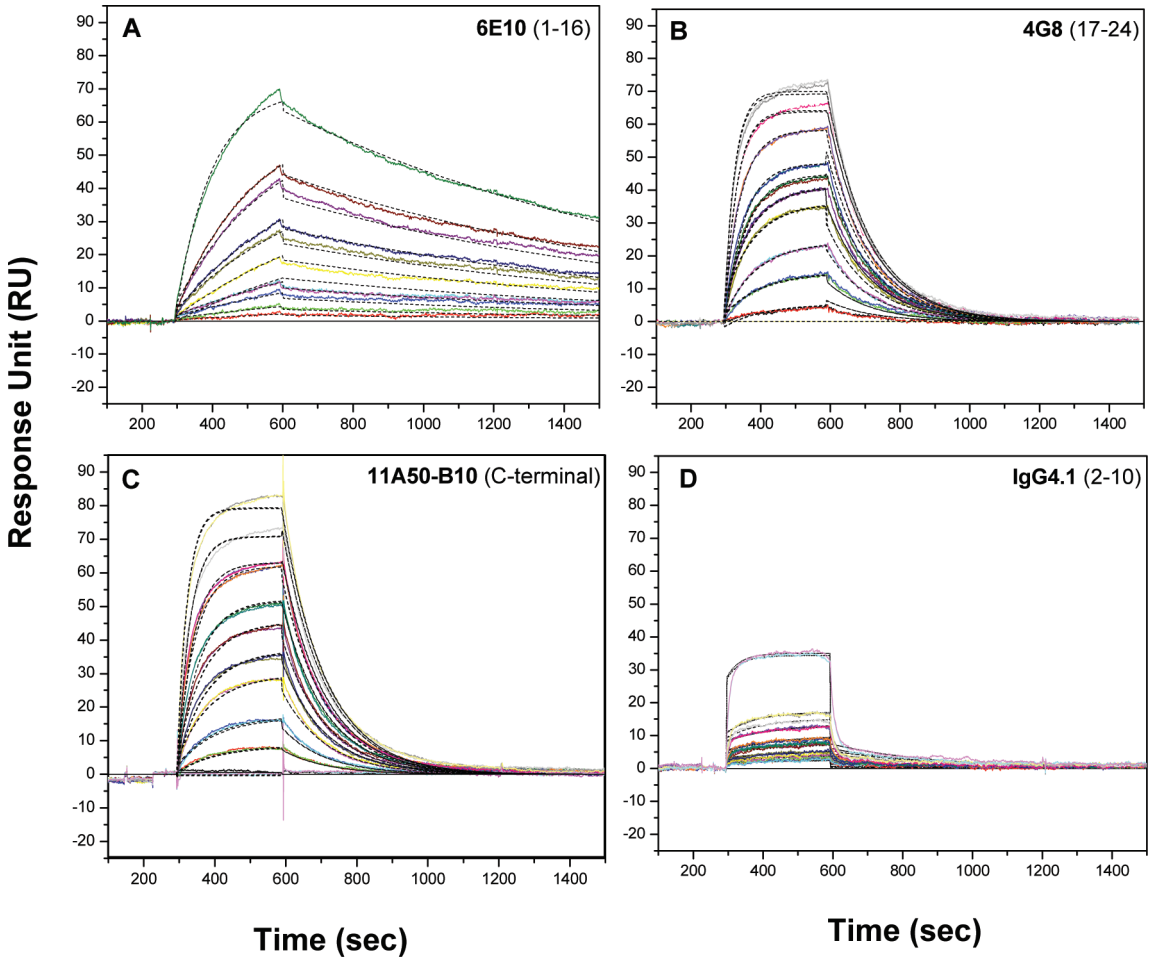

FIGURE 2: Kinetic analysis of Aβ monomers binding to immobilized antibodies. Kinetic analysis of different immobilized monoclonal antibodies IgG6E10 (A), IgG4G8 (B), IgG11A50 (C), and IgG4.1 (D) binding to monomeric Aβ40 at concentrations of 5, 10, 15, 20, 30, 40, 50, 75, 100, and 250 nM. The antibodies were immobilized at a ligand density of ~2000 Ru, and monomeric Aβ40 was injected for 5 min followed by a 15 min dissociation with HBS-EP buffer at a flow rate of 30 μL/min. The sensorgrams are shown as colored lines, and the fits are shown as black dashed lines. The kinetic parameters obtained from the fit are listed in Table 1.

region, generating F(ab) or F(ab′)$_2$ fragments without affecting the antigen binding regions. IgG4.1 was digested to the F(ab′)$_2$ fragment as described by Poduslo et al. (*13*), and the binding kinetics of both antibodies with monomeric and fibrillar Aβ40 were evaluated. Figure 1B shows the binding of IgG4.1 and F(ab′)$_2$4.1 at a single concentration of 200 nM to fibrillar Aβ40. The sensorgrams for binding of IgG4.1 and F(ab′)$_2$4.1 to monomeric Aβ40 at concentrations from 30 to 3000 nM and their theoretical fit are shown in panels C and D of Figure 1, respectively. The binding kinetics of the native antibody and digested antibody fragment F(ab′)$_2$4.1 are largely unaltered, with the binding regions being well-preserved following enzyme digestion. Similarly, the binding of the native IgG4.1 and F(ab′)$_2$4.1 fragments to immobilized Aβ40 fibrils showed nearly identical association curves and a slightly faster dissociation profile of F(ab′)$_2$4.1 compared to that of IgG4.1. Our earlier studies have demonstrated poor binding of Fab fragments to Aβ fibrils or amyloid plaques, whereas IgG4.1 and F(ab′)$_2$4.1 showed nearly identical binding to different forms of Aβ40 (*13*). Hence, Fab fragments were not used in this study.

Kinetic Analysis of Aβ Monomers Binding to Immobilized Antibodies. To study the kinetics of binding of different antibodies to monomeric Aβ40, the antibodies were immobilized at a density of ~2000 RU. A nonspecific antibody (L227- IgG1κ antibody produced by mouse myeloma L227, catalog no. HB-96, ATCC) was immobilized at a similar density over the reference surface to control nonspecific binding. Figure 2 depicts the experimental and theoretical fit of binding of different immobilized antibodies and their kinetics of binding. These profiles also show binding kinetics of association with and dissociation from freshly prepared monomeric Aβ40 at concentrations from 5 to 200 nM. The kinetic parameters obtained from the simultaneous 1:1 Langmuir fit of association and dissociation phases of all sensorgrams are given in Table 1. 6E10 and 4G8, which are standard mAbs used in immunohistochemistry, show very different kinetic patterns but a similar affinity for soluble monomeric Aβ40. 4G8 has a stronger ability to bind to monomeric Aβ40 with a higher association rate constant (k_a) of 26.8×10^4 M^{-1} s^{-1}, but its immune complex with Aβ40 tends to dissociate quickly with a low dissociation constant (k_d) of 0.81×10^{-4} s^{-1}. Moreover, the 4G8 antibody has an affinity of 30.1 nM for monomeric Aβ40, which is the ratio of the dissociation and association rates. In contrast, antibody 6E10 has an affinity of 22.3 nM with a slower association constant of 3.8×10^4 M^{-1} s^{-1}, but it forms a more stable immune complex than 4G8 and demonstrates a higher dissociation constant of 8.48×10^{-4} s^{-1}.

Peptide-capturing antibody 11A50 shows a kinetic pattern nearly similar to that of 4G8 with an affinity for monomeric Aβ40 of 32.5 nM (Figure 2C and Table 1). Surprisingly, its immune complex with Aβ40 is less stable with a quicker

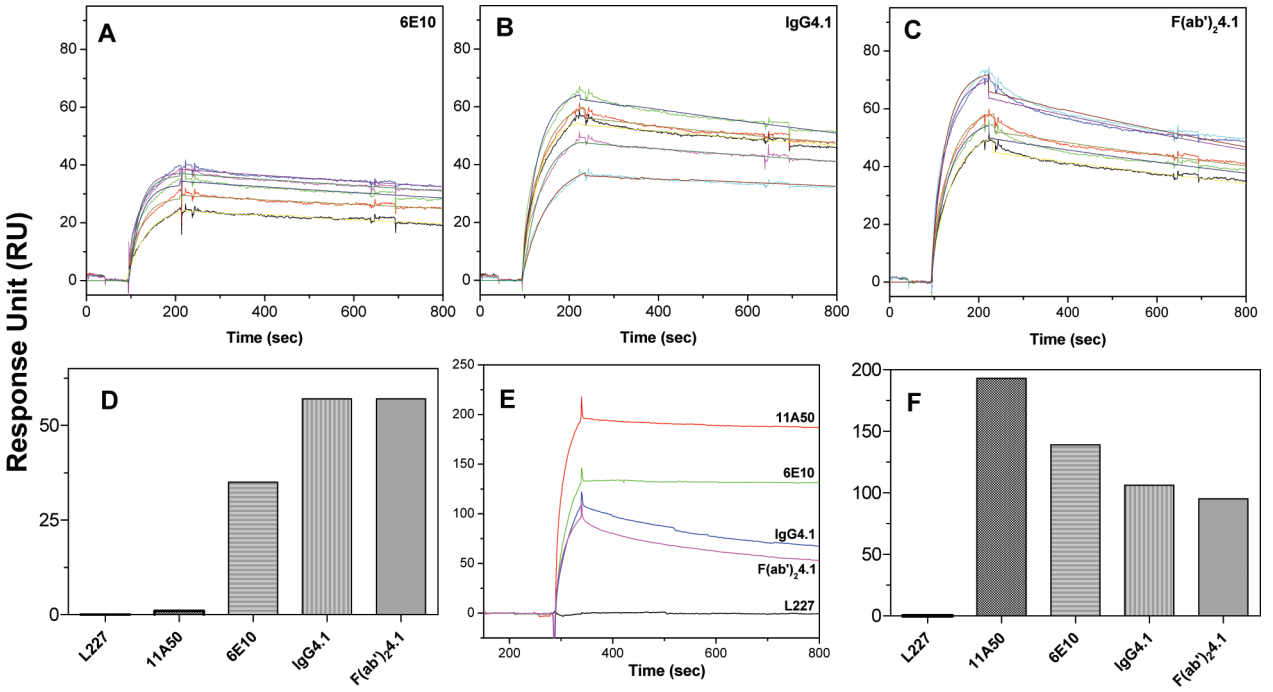

FIGURE 3: Kinetic analysis of antibody binding to immobilized sonicated Aβ40 fibrils. Kinetic analysis of 6E10 (A), IgG4.1 (B), and F(ab′)$_2$4.1 (C) binding to immobilized sonicated Aβ40 fibrils at 33, 66, 100, 166, and 200 nM. Sonicated Aβ40 fibrils were immobilized at a ligand density of 60 RU, and antibody samples were injected for 1 min followed by a 15 min dissociation with HBS-EP buffer at a flow rate of 30 μL/min. The sensorgrams are shown as colored lines, and the fits are shown as black lines. The kinetic parameters obtained from the fit are listed in Table 1. Panel D shows the bar chart of the peak binding response at the end of sample injection. In panel E, freshly prepared monomeric Aβ40 was immobilized at a ligand density of ~60 RU, and different antibodies were injected at a concentration of 67 nM. Panel F shows the bar chart of the peak binding response at the end of sample injection.

dissociation constant ($k_d = 0.80 \times 10^{-4}$ s^{-1}). IgG4.1, which is a plaque-binding mAb, shows specific binding to Aβ40 but with an extremely low affinity of 512 nM (Figure 2D and Table 1). The binding response at each concentration is also lower compared to those of other antibodies studied here, and it forms a less stable immune complex with a k_d of 0.037 s^{-1}. F(ab′)$_2$4.1 of IgG4.1 showed a kinetic profile similar to that of the native antibody with an affinity of 491 nM.

Kinetic Analysis of Antibody Binding to Immobilized Sonicated Aβ40 Fibrils. The sonicated Aβ40 fibrils are not suitable for use as an analyte for injection over the chip surface due to their heterogeneity. Hence, they were immobilized as a ligand over the chip surface using carbodiimide chemistry at a low density of 60 RU, and different concentrations of antibodies were injected as analytes at a flow rate of 30 μL/min. Panels A−C of Figure 3 depicts the Aβ40 fibril binding sensorgrams of 6E10, IgG4.1, and F(ab′)$_2$4.1, respectively, from 33 to 200 nM. The sensorgrams were reproducible at all concentrations studied, and there is not much change in the shape of the sensorgrams. However, plaque-binding antibodies IgG4.1 and F(ab′)$_2$4.1 exhibit enhanced binding to the fibrils compared to other antibodies studied. In addition, the sensorgrams of IgG4.1 and F(ab′)$_2$4.1 are nearly similar except that F(ab′)$_2$4.1 has a slightly quicker dissociation phase. Surprisingly, peptide-capturing antibody 11A50 did not exhibit any reliable binding to the fibrils, which indicates the C-terminal region of fibrillar Aβ40 may be buried inside the β-sheet fibril structure and hence unavailable for antibody 11A50. Alternatively, being a peptide-capturing antibody, it may have weak affinity for the fibrils.

The carbodiimide chemistry that was employed to immobilize the Aβ40 fibrils to the dextran matrix of the chip modifies the free NH_2 group from the N-terminal region and also the side chain lysine at positions 16 and 28 of Aβ40 fibrils. The absence of 4G8 binding to the immobilized Aβ40 fibrils might be due to the covalent modification at position 16, which could potentially block the epitope binding region of 4G8. The bar chart in Figure 3D shows the peak binding response of different antibodies binding to immobilized sonicated Aβ40 fibrils at the end of the sample injection (220 s). Clearly, the 6E10 and IgG4.1 antibodies, which are specific to the N-terminal region of the Aβ peptide, exhibit better binding. Plaque-binding antibody IgG4.1 and its F(ab′)$_2$4.1 fragment exhibit stronger binding than 6E10 does. Similar results were also observed when a very low density (~9 RU) of sonicated Aβ40 fibrils was immobilized (data not shown). L227, which is a nonspecific (negative control) antibody, did not exhibit any measurable binding response to Aβ40 fibrils. Since the shapes of the sensorgrams are nearly similar, kinetic analysis of these sensorgrams yields comparable affinity constants between 1 and 2.5 nM and nearly similar dissociation constants (Table 1).

Interaction of the injected antibody with the immobilized antigen involves some avidity effect in addition to the specific binding. If there is no avidity effect, injection of the antibodies onto the immobilized monomeric Aβ40 surface and vice versa should provide similar kinetics as shown in Figure 2. To evaluate this, we immobilized the monomeric Aβ40 at a ligand density of 60 RU and injected the chosen antibodies at a concentration of 67 nM (Figure 3E). The sensorgrams were different than those shown in Figure 2, which is most likely due to avidity. The binding response shown in Figure 3F illustrates some interesting trends with peptide-capturing antibody 11A50, which had the most avidity for monomeric Aβ40 followed by 6E10 and IgG4.1. Because each is a plaque-binding antibody, the avidity of IgG4.1

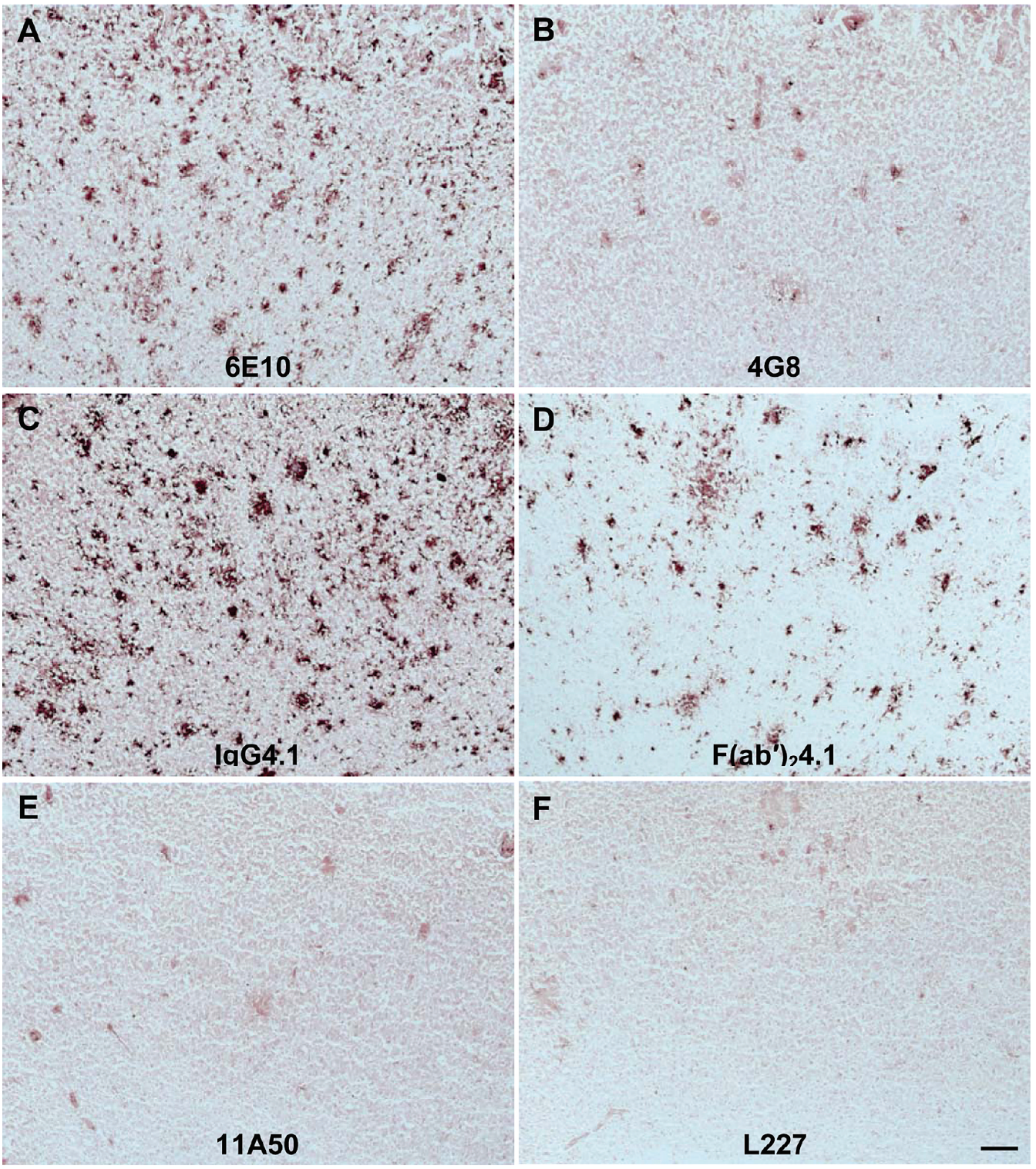

FIGURE 4: Labeling of amyloid plaques in APP mouse brain sections with 6E10, 4G8, IgG4.1, F(ab′)$_2$4.1, and L227. Sections (15 μm) of APP mouse brain incubated with 1.0 μg/mL anti-amyloid antibodies are illustrated as follows: (A) 6E10, (B) 4G8, (C) IgG4.1, (D) F(ab′)$_2$4.1, (E) 11A50, and (F) L227. The scale bar is 100 μm.

or F(ab′)$_2$4.1 is low; they bind to the monomeric Aβ40 and tend to dissociate quickly compared to 11A50 and 6E10.

The polyamine modification strategy has been employed to increase the BBB permeability of therapeutic or diagnostic proteins delivered to the brain (*12*−*14*). To study how the modification alters the antigen binding ability, pIgG4.1 or pF(ab′)$_2$4.1 was injected over the immobilized sonicated Aβ40 chip surface at different concentrations ranging from 33 to 200 nM. Clearly, pIgG4.1 (Figure 5A) and pF(ab′)$_2$4.1 (Figure 5B) show enhanced binding to sonicated fibrils, as compared to unmodified IgG4.1 and F(ab′)$_2$4.1 (Figure 3). Kinetic analysis of the sensorgrams demonstrates that the affinity constant (K_D) is not substantially altered compared to those of unmodified IgG4.1 and F(ab′)$_2$4.1 (see Table 1). The perceived change in the K_D arises from the small changes observed in the association (k_a) and dissociation (k_d) constants. In the case of IgG4.1, the polyamine

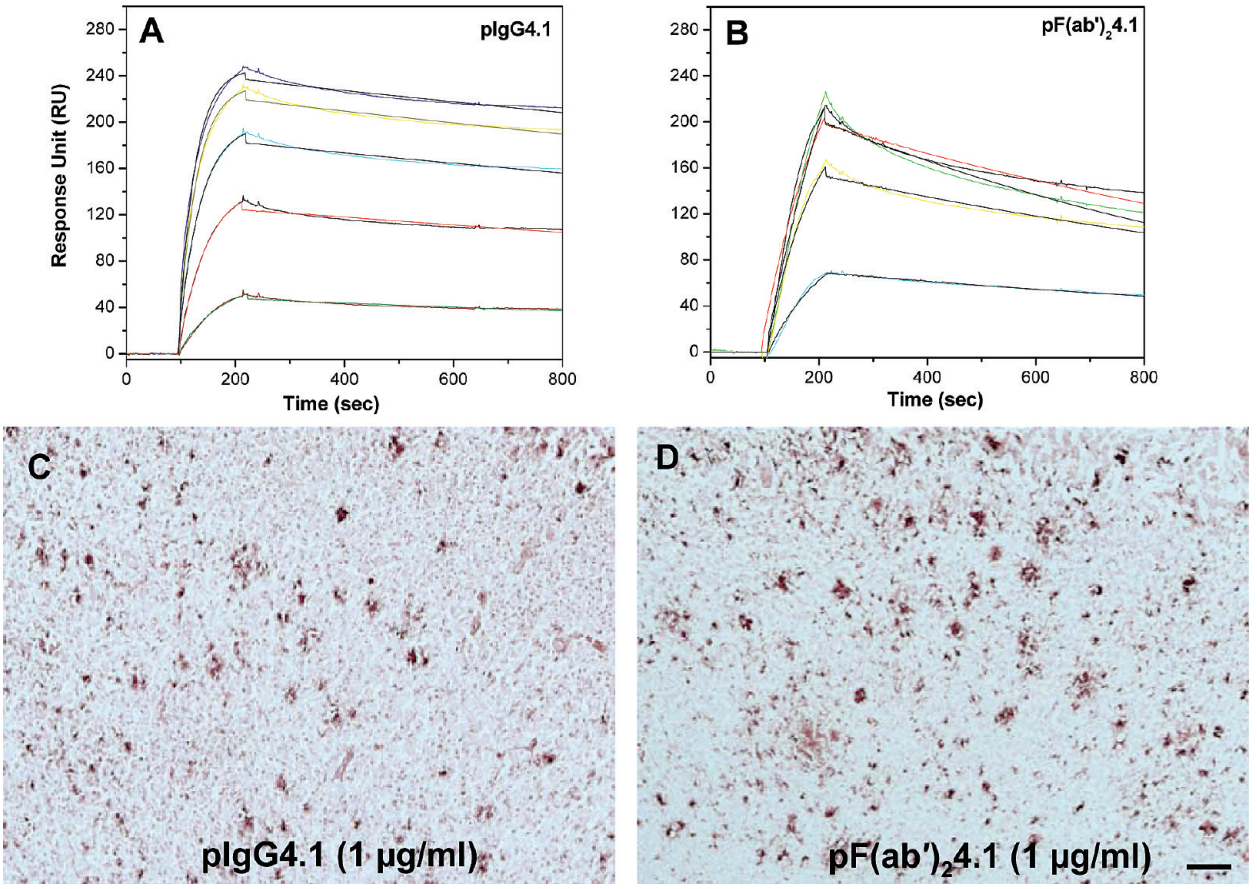

FIGURE 5: Kinetic analysis of Aβ40 fibril binding to pIgG4.1 (A) and pF(ab′)$_2$4.1 (B) at concentrations of 33, 66, 100, 166, and 200 nM. Labeling of amyloid plaques in APP mouse brain sections with pIgG4.1 (C) and pF(ab′)$_2$4.1 (D). The scale bar is 100 μm.

modification increases the association rate from 18.5×10^4 to 28.7×10^4 M^{-1} s^{-1} without a significant change in the dissociation rate. However, with pF(ab′)$_2$4.1, the association rate decreased from 22.4×10^4 to 15.8×10^4 M^{-1} s^{-1}, and the dissociation rate decreased from 5.34×10^{-4} to 3.35×10^{-4} s^{-1}. Since both IgG4.1 and F(ab′)$_2$4.1 have weak affinities for monomeric Aβ40, we did not further study the kinetics of binding of pIgG4.1 and pF(ab′)$_2$4.1 to monomeric Aβ40.

Labeling of Amyloid Plaques in APP Mouse Brain Sections with 6E10, 4G8, IgG4.1, F(ab′)$_2$4.1, pIgG4.1, pF(ab′)$_2$4.1, and L227. The plaque labeling of different anti-amyloid antibodies (6E10, 4G8, IgG4.1, F(ab′)$_2$4.1, and L227) in APP transgenic mouse brain sections is illustrated in Figure 4. Sections (15 μm) of APP mouse brain were incubated with anti-amyloid antibodies at a concentration of 1 or 0.5 μg/mL. The level of plaque labeling increased with increasing antibody concentrations from 0.5 to 1 μg/mL. Antibody 11A50 exhibited much lower immunoreactivity than the other antibodies (Figure 4E). This is most likely due to the weak affinity for amyloid plaques; it also binds to only Aβ1−40 while the other antibodies bind to both Aβ1−40 and Aβ1−42. The nonspecific control antibody (L227) did not exhibit any binding to amyloid plaques (Figure 4F). Polyamine modification of either IgG4.1 or F(ab′)$_2$4.1 did not have a substantial effect on plaque labeling (Figure 5C,D).

The normalized densitometry of the immunoreactivity of anti-amyloid antibody with respect to amyloid plaques in APP transgenic mouse brain sections is plotted in Figure 6. Lower grayscale values and ratios represent darker shades of gray and black due to higher levels of immunoreactivity and antibody

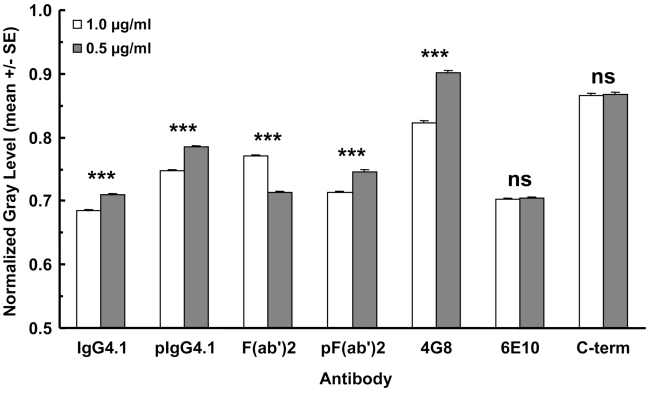

FIGURE 6: Densitometry of 6E10, 4G8, IgG4.1, F(ab′)$_2$4.1, and L227 labeling of amyloid plaques in APP mouse brain sections. The ordinate plots the normalized grayscale values as a mean of the plaques analyzed for each antibody and concentration. The error bars indicate the standard error of the mean. The anti-amyloid antibodies are listed along the abscissa. For each antibody, the left bar represents a concentration of 1.0 μg/mL and the right bar a concentration of 0.5 μg/mL. ANOVA (two-way): antibody [$F(6,10877) = 809.5$; $p < 0.0001$], concentration [$F(1,10877) = 80.52$; $p < 0.0001$], and interaction [$F(6,10877) = 73.99$; $p < 0.0001$]. Bonferroni post hoc multiple comparisons: $p < 0.0001$ (asterisks).

binding. The grayscale values were normalized by dividing them by the grayscale value of an ROI measured on the empty slide immediately adjacent to the brain section, resulting in ratios of < 1. The standard error bars are small because of the large number of plaques analyzed for each antibody. The lower concentration of antibody resulted in lower levels of immunoreactivity,

which translated into higher ratios. When the concentration of the antibody was halved, the differences were statistically significant, but the differences in immunoreactivity were not substantial. This is probably due to the high affinity of the antibodies, which is typical for antibodies in general.

DISCUSSION

The aim of this study was to investigate the kinetics of binding of different anti-amyloid monoclonal antibodies to monomeric and fibrillar Aβ40 using a surface plasmon resonance technique and their plaque binding ability with transgenic AD mouse brain sections using immunohistochemistry. The motivation here is to understand the various biophysical factors governing the efficacy of anti-amyloid antibodies used for different purposes in Alzheimer's research. The knowledge gained from this study would be helpful in selecting a potential antibody for AD research and/or clinical applications.

The results clearly indicate that the antibodies studied exhibit characteristic kinetics of binding to monomeric and fibrillar Aβ40 and an ability to bind amyloid plaques that are germane to the antibody itself. The kinetics of binding of various antibodies to Aβ40 monomers followed the Langmuir model, although IgG4.1 and F(ab′)$_2$4.1 showed some degree of heterogeneity with a rapid exponential dissociation phase. However, the kinetics of binding of an antibody to Aβ40 fibrils is confounded by avidity to yield true kinetics. The terms affinity and avidity are distinct; affinity refers to the strength of a single interaction, and avidity describes the combined strength of multiple interactions between the antibody and antigen. For example, IgM may have a low or high affinity depending on the antigen, but its avidity is higher than that of IgG because of the availability of 10 binding sites which contrast with the two binding sites of IgG. When IgG mAb is immobilized as a ligand to the sensor surface and monomeric antigen is injected as an analyte, the major interaction could be affinity without a substantial avidity effect. However, when the monomeric or heterogeneous antigen is immobilized as a ligand and the IgG is injected as an analyte, the interactions with the immobilized antigen involve more avidity. It is conceivable that the simple 1:1 Langmuir model may not adequately reflect the multiphasic binding kinetics between Aβ protein and the antibodies. Most of these multiphasic interactions could emerge from the interactions between neighboring antibodies from the sensor surface or be due to increased analyte concentrations. To weaken the impact of the multiphasic interactions, we immobilized a low density of ligands on the chip surface and also used low analyte concentrations. As a result, the Langmuir model fit the data reasonably well with good residual plots and acceptable χ^2 values. Use of other complex models available in Bioevaluation did not improve the fit significantly.

IgG4.1 is a novel plaque-binding monoclonal antibody, raised against the fibrillar human Aβ42 to target AD amyloid plaques for imaging and therapeutic purposes for AD. IgG4.1 shows more avidity for Aβ40 fibrils and labels dense core plaques but shows less affinity (~512 nM) for soluble monomeric Aβ40. Ficin enzyme digestion of IgG4.1 to F(ab′)$_2$4.1 did not affect the antigen binding regions. Earlier, we (*13*) reported that the polyamine modification of IgG4.1 or F(ab′)$_2$4.1 increases the BBB permeability by ~50- or ~25-fold, respectively. In addition, we have successfully targeted the amyloid plaques by intravenous administration of pIgG4.1 and pF(ab′)$_2$4.1 in AD transgenic animals. We found that native IgG4.1 and pIgG4.1 also label amyloid deposits present in blood vessels. In line with these observations, the affinity constant (K_D) for binding of pIgG4.1 and pF(ab′)$_2$4.1 to sonicated Aβ40 fibrils derived from SPR analysis remains similar to that for unmodified IgG4.1 and F(ab′)$_2$4.1 (Table 1). In addition to the fibril binding, its plaque binding ability in AD transgenic mouse brain sections was also not significantly altered (Figures 5 and 6). These data confirm the utility of using pIgG4.1 or pF(ab′)$_2$4.1 as a plaque-targeting antibody for molecular imaging.

Recently, Seubert et al. (*11*) reported that 3D6, a plaque-binding antibody, is effective in reducing the size of the amyloid plaque burden in AD mice, whereas m266, a peptide-capturing antibody, not only is ineffective in reducing the size of the amyloid plaque burden but also increases the vascular level of amyloid. The same group reported that the 3D6 antibody shows an affinity for soluble Aβ42 of 2.4 nM, determined by surface plasmon resonance studies (*24*). Our plaque binding antibody IgG4.1 shows preferential affinity for fibrillar Aβ40 (1.5 nM) versus monomeric Aβ40 (512 nM). It is interesting to compare the IgG4.1 antibody to a conformational specific antibody reported by Kayed et al. (*25*) which was raised like IgG4.1 by immunization with homogeneous Aβ42 fibrils. Interestingly, this antibody specifically binds to β-sheet fibrillar forms of different amyloidogenic proteins such as Aβ, α-synuclein, and transthyrin but not to the unstructured monomeric or oligomeric forms in a sequence-independent manner.

The peptide-capturing antibody, 11A50, which is specific to the C-terminal region of Aβ40, shows an affinity for Aβ40 of 32.5 nM but did not show any specific binding to the immobilized fibrils or to the amyloid plaques in AD mouse brain slices. The poor binding to the fibrils may be due to the burial of the Aβ binding site inside the β-sheet fibrillar structure or due to the low levels of Aβ40 present in mouse tissue sections. In contrast, m266 is another peptide-capturing antibody with a high k_a of 3.1×10^7 M^{-1} s^{-1}, a k_d of 0.9×10^{-4} s^{-1}, and an extremely high affinity of 2.8 pM for the soluble Aβ peptide (*26*). There are several peptide-capturing mAbs that are commercially available for basic science, but it is beyond the scope of this study to compare and contrast their biophysical properties with those of 11A50. It is certainly beneficial to know the affinity of the antibodies so that an appropriate antibody can be chosen to suit the bioanalytical experiment. While m266 is not commercially available, for example, for comparison of the affinities of 11A50 and m266, the high affinity of m266 (2.8 pM) for the soluble Aβ peptide makes it a better choice than 11A50 for capturing soluble Aβ from complex biological samples.

6E10 and 4G8 are standard monoclonal antibodies used in immunohistochemistry for dense core and diffuse plaque labeling, respectively. In addition, these antibodies are also widely used for Aβ peptide capturing in various bioanalytical experiments such as ELISA, Western blot, immunoprecipitation, etc. Recently, it was reported that the dense core plaques have more fibrillar structure with β-sheet secondary structures, whereas the diffuse plaques are amorphous deposits without any ordered structure (*27*). The affinities of 6E10 and 4G8 for Aβ40 are nearly similar, but both exhibit different kinetics as shown in Figure 2. Immunohistochemistry followed by densitometry analysis of the plaque labeling shows that 6E10 and IgG4.1 bind to plaques equally well. While the fibril binding kinetic data of 4G8 are hard to obtain from the SPR studies due to the chemistry employed to immobilize the fibrils to the chip surface, its immunohistochemistry demonstrates weaker plaque binding compared to 6E10 and

IgG4.1. The higher k_a of 26.8×10^4 M^{-1} s^{-1} for 4G8 binding to monomeric Aβ may be translated to its better binding to diffuse plaques, which has more randomly structured Aβ peptides. Similarly, the slower binding of 6E10 ($k_a = 3.8 \times 10^4$ M^{-1} s^{-1}) to monomeric Aβ40 may be responsible for its ability to bind Aβ40 fibrils (Figure 3), and the higher amyloid plaque binding immunoreactivity observed in the densitometry plaque binding analysis (Figure 6). These results also correlate with a recent study in which it was demonstrated that systemic and prolonged intracerebroventricular administration of the 6E10 antibody reduced amyloid plaque burden in old AD transgenic mice brain (*28*).

Antibody−antigen interactions are highly specific. The Aβ peptides exist in morphologically different forms such as monomer, oligomer, fibrils, etc. On the basis of the solid state NMR structure of Aβ amyloid fibrils, the first 10 residues of Aβ40 are structurally disordered, while residues 12−24 and 30−40 adapt β-strand conformations and form parallel β-sheets through intermolecular hydrogen bonding (*4*). It can be said, on the basis of this structural model, that IgG4.1 was raised against the flexible region of the fibrillar Aβ peptide. In addition, the epitope region of IgG4.1, Aβ2−10, also overlaps the immunodominant region (AEFRHD) of Aβ2−7. Interestingly, a Blast search of the entire human genome with AEFRHD provides the amyloid precursor protein as the only hit that has the same sequence. Also, when AD patients were actively immunized with fibrillar Aβ42 peptides with adjuvants, the patients produced polyclonal antibodies which are predominantly specific to the amino terminus of the Aβ peptide (*29*). Thakker et al. (*28*) reported that the Aβ binding properties of these antibodies are similar to those of 6E10, but there is not much information available. Understanding the kinetic details of those endogenous polyclonal antibodies may provide critical information about the development of a valid antibody for AD passive immunotherapy. Recently, Shankar et al. (*5*) reported that only the antibodies specific for the amino terminus, and not the C-terminus of Aβ, are effective in preventing long-term potentiation and long-term depression of neurons in AD mouse hippocampal slices when the antibodies were co-injected with the toxic Aβ oligomers isolated from the AD human brain.

Clearly, there has been good progress in AD passive immunization research which is moving forward with more focus on N-terminal monoclonal antibodies raised against the N-terminal region of amyloid peptides. While 3D6 and m266 were raised by immunization of covalently coupled Aβ fragments to sheep anti-mouse IgG, IgG4.1 and the conformational specific antibody discussed above were developed by immunization of Aβ42 fibrils alone. Antibodies IgG4.1 and 6E10 bind specifically to the N-terminal region of the Aβ peptide, and both the antibodies bind to monomeric as well as fibrillar Aβ40 (Figures 2, 3, and 6). This bivalent binding may be due to the availability of the N-terminal region of the Aβ peptide in different conformations. In addition, the affinity for monomeric Aβ40 is significantly higher for 6E10 than IgG4.1. A single peripheral administration of plaque-binding antibody 3D6 in transgenic mice increased plasma Aβ40−42 levels by 6−9-fold, whereas peptide-capturing antibody m266 increased plasma Aβ levels dramatically by 80−100-fold. Similarly, with 6E10, an approximately 6−7-fold increase in the plasma Aβ peptide level has been documented (*28*, *30*). It will be useful to conduct similar studies with IgG4.1, which has a low affinity for monomeric Aβ40 but higher avidity for fibrillar Aβ40, and develop a predictive pharmacodynamic model by combining the kinetic constants obtained from surface plasmon resonance with the pharmacodynamic response of single peripheral antibody administration. Increasing the level of delivery of the antibody across the BBB even by trace amounts without affecting the antigen binding properties by the polyamine modification strategy might increase the therapeutic or diagnostic potential of the antibody (*13*). In brief, antibodies remain an indispensible tool for both basic and clinical AD research; hence, new and faster ways are required to screen antibodies for specific uses. As demonstrated in this study, surface plasmon resonance and immunohistochemistry may provide a rationale for screening potential anti-Aβ mAbs for various purposes.

REFERENCES

1. Selkoe, D. J. (2001) Alzheimer's disease: Genes, proteins, and therapy. *Physiol. Rev. 81*, 741–766.
2. Paravastu, A. K., Leapman, R. D., Yau, W. M., and Tycko, R. (2008) Molecular structural basis for polymorphism in Alzheimer's β-amyloid fibrils. *Proc. Natl. Acad. Sci. U.S.A. 105*, 18349–18354.
3. Petkova, A. T., Leapman, R. D., Guo, Z., Yau, W. M., Mattson, M. P., and Tycko, R. (2005) Self-propagating, molecular-level polymorphism in Alzheimer's β-amyloid fibrils. *Science 307*, 262–265.
4. Tycko, R. (2006) Molecular structure of amyloid fibrils: Insights from solid-state NMR. *Q. Rev. Biophys. 39*, 1–55.
5. Shankar, G. M., Li, S., Mehta, T. H., Garcia-Munoz, A., Shepardson, N. E., Smith, I., Brett, F. M., Farrell, M. A., Rowan, M. J., Lemere, C. A., Regan, C. M., Walsh, D. M., Sabatini, B. L., and Selkoe, D. J. (2008) Amyloid-β protein dimers isolated directly from Alzheimer's brains impair synaptic plasticity and memory. *Nat. Med. 14*, 837–842.
6. Lesne, S., Koh, M. T., Kotilinek, L., Kayed, R., Glabe, C. G., Yang, A., Gallagher, M., and Ashe, K. H. (2006) A specific amyloid-β protein assembly in the brain impairs memory. *Nature 440*, 352–357.
7. Bard, F., Cannon, C., Barbour, R., Burke, R. L., Games, D., Grajeda, H., Guido, T., Hu, K., Huang, J., Johnson-Wood, K., Khan, K., Kholodenko, D., Lee, M., Lieberburg, I., Motter, R., Nguyen, M., Soriano, F., Vasquez, N., Weiss, K., Welch, B., Seubert, P., Schenk, D., and Yednock, T. (2000) Peripherally administered antibodies against amyloid β-peptide enter the central nervous system and reduce pathology in a mouse model of Alzheimer's disease. *Nat. Med. 6*, 916–919.
8. Foster, J. K., Verdile, G., Bates, K. A., and Martins, R. N. (2008) Immunization in Alzheimer's disease: Naive hope or realistic clinical potential? *Mol. Psychiatry 14*, 239–251.
9. Nitsch, R. M., and Hock, C. (2008) Targeting β-amyloid pathology in Alzheimer's disease with Aβ immunotherapy. *Neurotherapeutics 5*, 415–420.
10. DeMattos, R. B., Bales, K. R., Cummins, D. J., Dodart, J. C., Paul, S. M., and Holtzman, D. M. (2001) Peripheral anti-Aβ antibody alters CNS and plasma Aβ clearance and decreases brain Aβ burden in a mouse model of Alzheimer's disease. *Proc. Natl. Acad. Sci. U.S.A. 98*, 8850–8855.
11. Seubert, P., Barbour, R., Khan, K., Motter, R., Tang, P., Kholodenko, D., Kling, K., Schenk, D., Johnson-Wood, K., Schroeter, S., Gill, D., Jacobsen, J. S., Pangalos, M., Basi, G., and Games, D. (2008) Antibody capture of soluble Aβ does not reduce cortical Aβ amyloidosis in the PDAPP mouse. *Neurodegener. Dis. 5*, 65–71.
12. Ramakrishnan, M., Wengenack, T. M., Kandimalla, K. K., Curran, G. L., Gilles, E. J., Ramirez-Alvarado, M., Lin, J., Garwood, M., Jack, C. R., Jr., and Poduslo, J. F. (2008) Selective contrast enhancement of individual Alzheimer's disease amyloid plaques using a polyamine and Gd-DOTA conjugated antibody fragment against fibrillar Aβ42 for magnetic resonance molecular imaging. *Pharm. Res. 25*, 1861–1872.
13. Poduslo, J. F., Ramakrishnan, M., Holasek, S. S., Ramirez-Alvarado, M., Kandimalla, K. K., Gilles, E. J., Curran, G. L., and Wengenack, T. M. (2007) In vivo targeting of antibody fragments to the nervous system for Alzheimer's disease immunotherapy and molecular imaging of amyloid plaques. *J. Neurochem. 102*, 420–433.
14. Poduslo, J. F., Curran, G. L., and Berg, C. T. (1994) Macromolecular permeability across the blood-nerve and blood-brain barriers. *Proc. Natl. Acad. Sci. U.S.A. 91*, 5705–5709.
15. Abdullah, L., Paris, D., Luis, C., Quadros, A., Parrish, J., Valdes, L., Keegan, A. P., Mathura, V., Crawford, F., and Mullan, M. (2007) The influence of diagnosis, intra- and inter-person variability on serum and plasma Aβ levels. *Neurosci. Lett. 428*, 53–58.

16. Ertekin-Taner, N., Younkin, L. H., Yager, D. M., Parfitt, F., Baker, M. C., Asthana, S., Hutton, M. L., Younkin, S. G., and Graff-Radford, N. R. (2008) Plasma amyloid β protein is elevated in late-onset Alzheimer's disease families. *Neurology 70*, 596–606.
17. Ringman, J. M., Younkin, S. G., Pratico, D., Seltzer, W., Cole, G. M., Geschwind, D. H., Rodriguez-Agudelo, Y., Schaffer, B., Fein, J., Sokolow, S., Rosario, E. R., Gylys, K. H., Varpetian, A., Medina, L. D., and Cummings, J. L. (2008) Biochemical markers in persons with preclinical familial Alzheimer's disease. *Neurology 71*, 85–92.
18. Agyare, E. K., Curran, G. L., Ramakrishnan, M., Yu, C. C., Poduslo, J. F., and Kandimalla, K. K. (2008) Development of a smart nano-vehicle to target cerebrovascular amyloid deposits and brain parenchymal plaques observed in Alzheimer's disease and cerebral amyloid angiopathy. *Pharm. Res. 25*, 2674–2684.
19. Hsiao, K., Chapman, P., Nilsen, S., Eckman, C., Harigaya, Y., Younkin, S., Yang, F., and Cole, G. (1996) Correlative memory deficits, Aβ elevation, and amyloid plaques in transgenic mice. *Science 274*, 99–102.
20. Wengenack, T. M., Whelan, S., Curran, G. L., Duff, K. E., and Poduslo, J. F. (2000) Quantitative histological analysis of amyloid deposition in Alzheimer's double transgenic mouse brain. *Neuroscience 101*, 939–944.
21. Bitan, G., and Teplow, D. B. (2005) Preparation of aggregate-free, low molecular weight amyloid-β for assembly and toxicity assays. *Methods Mol. Biol. 299*, 3–9.
22. Nichols, M. R., Moss, M. A., Reed, D. K., Lin, W. L., Mukhopadhyay, R., Hoh, J. H., and Rosenberry, T. L. (2002) Growth of β-amyloid-(1−40) protofibrils by monomer elongation and lateral association. Characterization of distinct products by light scattering and atomic force microscopy. *Biochemistry 41*, 6115–6127.
23. Langmuir, I. (1918) The adsorption of gases on plane surfaces of glass, mica and platinum. *J. Am. Chem. Soc. 40*, 1361–1404.
24. Tsurushita, N., and Vasquez, M. J., US Patent No. 7,318,923 B2.
25. Kayed, R., Head, E., Sarsoza, F., Saing, T., Cotman, C. W., Necula, M., Margol, L., Wu, J., Breydo, L., Thompson, J. L., Rasool, S., Gurlo, T., Butler, P., and Glabe, C. G. (2007) Fibril specific, conformation dependent antibodies recognize a generic epitope common to amyloid fibrils and fibrillar oligomers that is absent in prefibrillar oligomers. *Mol. Neurodegener. 2*, 18.
26. Davies, J., Tang, Y., and Watkins, J. D. US Patent No. US 2006/0110388 A1.
27. Rak, M., Del Bigio, M. R., Mai, S., Westaway, D., and Gough, K. (2007) Dense-core and diffuse Aβ plaques in TgCRND8 mice studied with synchrotron FTIR microspectroscopy. *Biopolymers 87*, 207–217.
28. Thakker, D. R., Weatherspoon, M. R., Harrison, J., Keene, T. E., Lane, D. S., Kaemmerer, W. F., Stewart, G. R., and Shafer, L. L. (2009) Intracerebroventricular amyloid-β antibodies reduce cerebral amyloid angiopathy and associated micro-hemorrhages in aged Tg2576 mice. *Proc. Natl. Acad. Sci. U.S.A. 106*, 4501–4506.
29. Lee, M., Bard, F., Johnson-Wood, K., Lee, C., Hu, K., Griffith, S. G., Black, R. S., Schenk, D., and Seubert, P. (2005) Aβ42 immunization in Alzheimer's disease generates Aβ N-terminal antibodies. *Ann. Neurol. 58*, 430–435.
30. Gray, A. J., Sakaguchi, G., Shiratori, C., Becker, A. G., LaFrancois, J., Aisen, P. S., Duff, K., and Matsuoka, Y. (2007) Antibody against C-terminal Aβ selectively elevates plasma Aβ. *NeuroReport 18*, 293–296.